International Journal of Bifurcation and Chaos, Vol. 18, No. 8 (2008) 2169–2189

SYNTHESIS OF PIECEWISE-LINEAR CHAOTIC MAPS: INVARIANT DENSITIES, AUTOCORRELATIONS, AND SWITCHING

ALAN ROGERS*
Operation Studies Group, EirGrid Plc.,
160 Shelbourne Road, Dublin 4, Ireland
alan.rogers@eirgrid.com

ROBERT SHORTEN
Hamilton Institute, NUI Maynooth,
Maynooth, Co. Kildare, Ireland

DANIEL M. HEFFERNAN
Department of Mathematical Physics,
NUI Maynooth, Maynooth, Co. Kildare, Ireland

DAVID NAUGHTON
Department of Electronic Engineering,
NUI Maynooth, Maynooth, Co. Kildare, Ireland

Received June 19, 2006; Revised June 7, 2007

In this paper, we give a review of the Inverse Frobenius–Perron problem (IFPP): how to create chaotic maps with desired invariant densities. After describing some existing methods for solving the IFPP, we present a new and simple matrix method of doing this. We show how the invariant density and the autocorrelation properties of the maps can be controlled independently. We also give some fundamental results on switching between a number of different chaotic maps and the effect this has on the overall invariant density of the system. The invariant density of the switched system can be controlled by varying the probabilities of choosing each individual map. Finally, we present an interesting application of the matrix method to image generation, by synthesizing a two-dimensional map, which when iterated, generates a well-known image.

Keywords: Chaos; chaotic maps; chaos applications; Inverse Frobenius–Perron problem; IFPP.

1. Introduction

There has been increasing interest in recent years in the area of chaos control. Chaos control can refer to the stabilization of unstable orbits, such as in the seminal work of Ott *et al.* [1990], but it can also refer to controlling the statistical properties of chaotic systems [Chen & Dong, 1997]. Inverse Frobenius–Perron Problem (IFPP) refers to the problem of controlling the invariant densities of chaotic maps [Lasota & Mackey, 1994] (or synthesizing maps with prescribed invariant densities). The invariant density describes the statistical distribution of iterates in the state-space. A number of different approaches to this problem have appeared in

*Author for correspondence

the literature, including conjugate function-based, control-based, and matrix-based approaches [Grossmann & Thomae, 1977; Bollt, 2000; Gora & Boyarsky, 1993], as well as direct solutions of the Frobenius–Perron equation such as the work of Pingel *et al.* [1999]. Bollt [2000] gave a neat summary of the previous work on the topic. The IFPP may be viewed as a stepping-stone to new applications of chaos, which may flourish as new systematic synthesis and control techniques become available. Applications, therefore, are the main motivation behind this work. It is only when we have full control over a phenomenon, that we will be able to fully utilize it. Readers will be aware of applications of chaos in secure communications and various other ideas generally related to cryptography [Kocarev, 2001; Pareschi *et al.*, 2006]. Are there other areas which could benefit from some added chaos? We do not know the answer to this, but we believe that having systematic and straightforward procedures for generating and controlling chaos should make it easier for chaos to find applications, especially with nonspecialists in the area.

We recently developed a straightforward matrix approach to the IFPP which is completely mechanical, requiring little effort to generate a chaotic map with a desired invariant density. This work has potential applications in data modeling [Boyarsky & Góra, 2002] and creating random numbers with desired statistics, and was first described in [Rogers *et al.*, 2004]. A longer exposition of the method appeared in [Rogers *et al.*, 2008]. In this article, we shall describe in some detail the Inverse Frobenius–Perron problem, and describe existing methods of solving it. We then describe the new matrix method of solving the IFPP and then look at the autocorrelation properties of the maps. We show that variation of some key parameters can be used to control the rate of autocorrelation decay. We then consider the effect of switching between a number of alternative maps at each time step. For the class of chaotic maps we consider, the overall invariant density of the switched system is a weighted sum of the individual invariant densities. Finally, we show how the method can be used to synthesize two-dimensional and higher-dimensional maps, and illustrate the idea by creating a two-dimensional map which has an image encoded into its invariant density. Iteration of the maps leads to the image gradually emerging.

2. Background to the Inverse Frobenius–Perron Problem

The main tool used to analyze the statistical properties of chaotic maps is the Frobenius–Perron operator (FPO). The Inverse Frobenius–Perron problem (IFPP) is the technical name given to the synthesis problem: how to find a map that has a prespecified invariant density. There are several approaches to this problem in the literature, and they will be discussed along with the FPO in this section. The IFPP is interesting in both theoretical and practical ways. Theoretically, it is interesting that there is a method, indeed several methods, for controlling the invariant density of a map, and this is of practical use in areas such as the modeling of data (see [Boyarsky & Góra, 2002]). There are several key references on the FPO, the most notable being the book by Lasota and Mackey [1994]. The background material in this section is quite well known.

Normally, when we iterate a chaotic map on a computer starting from some initial condition x_0, the iterates fall chaotically on some attractor. It may be difficult to see the attractor if we just look at the time-series of the iterates. If we partition the state space into a series of bins, and count the fraction of iterates in each bin, a statistical picture of the chaotic attractor emerges. For almost all initial conditions (with respect to Lebesgue measure), the same picture emerges: a unique invariant density $\rho(x)$. It is true that for certain initial conditions (a set of points of Lebesgue measure zero made up of rational numbers, or extreme points) other invariant densities are possible, but for the maps we will be considering, there will be only one physically relevant invariant density [Schuster, 1989]. This density is stable if a small amount of noise is added to the system. In order to characterize the density mathematically, we consider an ensemble of initial conditions described by a probability density function $\rho_0(x)$ and observe how it changes as the entire ensemble is iterated. Eventually, the invariant density is reached, after, say n iterates. Further iteration of the ensemble of points just gives the invariant density $\rho(x)$ each time. The collection of initial conditions reaches a stable fixed-point. We now define the Frobenius–Perron operator, P, which is a linear operator acting on distributions of points:

$$\rho_{n+1} = P\rho_n \tag{1}$$

2.1. *The Frobenius–Perron equation*

The invariant density is a fixed point of the Frobenius–Perron operator (FPO). More formally, consider the iterates of some one-dimensional map, $f(x)$. An initial condition x_0 will map to $f(x_0)$, and a delta-function distribution $\delta(x - x_0)$ will map to $\delta(x - f(x_0))$ after one iteration. Now, utilizing the sifting property of delta functions,

$$\int f(x)\delta(x - x_0)dx = f(x_0) \tag{2}$$

we get the following relationship:

$$\delta(x - f(x_0)) = \int_0^1 \delta(x - f(y))\delta(y - x_0)dy \tag{3}$$

Now we simply replace the $\delta(y - x_0)$ with the more general $\rho_n(x)$, some arbitrary density after n iterations of $f(x)$, to get the Frobenius–Perron equation:

$$\rho_{n+1}(x) = \int_0^1 \rho_n(x)\delta(x - f(y))dy \tag{4}$$

The invariant density $\rho(x)$ is a fixed point of Eq. (4), and so we get:

$$\rho(x) = \int_0^1 \rho(x)\delta(x - f(y))dy \tag{5}$$

The Frobenius–Perron equation governs the time evolution of some arbitrary distribution of initial conditions $\rho_n(x)$ under some mapping $f(x)$. We shall only be concerned with mappings on the unit interval (hence the limits of integration in the above equations). Equation (4) is not particularly useful in itself. We now show how to recast it in a usable form.

2.2. *The Frobenius–Perron operator in explicit form*

Consider some one-dimensional map f acting on the unit interval, and an arbitrary subset of the state-space, A. Let ρ_n and ρ_{n+1} be densities at time steps n and $n+1$, respectively. From conservation of probability, we can write that:

$$\int_A \rho_{n+1}(x)dx = \int_{A'} \rho_n(x)dx \tag{6}$$

The right-hand integral must consist of all points mapped to A under one iteration of the map. Therefore A' is the preimage of A under the mapping f. We denote the preimage of A as $A' = f^{-1}(A)$. Suppose A is an interval contained in $[0, 1]$ of the form $A = [a, x]$. A may have many preimages under the mapping f. Equation (6) can be written as:

$$\int_a^x \rho_{n+1}(y)dy = \int_{f^{-1}([a,x])} \rho_n(y)dy \tag{7}$$

Now take the derivative with respect to x to get:

$$\rho_{n+1}(x) = \frac{d}{dx}\int_{f^{-1}([a,x])} \rho_n(y)dy \tag{8}$$

Finally, the invariant density will be a fixed point of this equation, so we drop the subscripts to get:

$$P\rho(x) = \frac{d}{dx}\int_{f^{-1}([a,x])} \rho(y)dy \tag{9}$$

Equation (9) is the most common form of the FPO. For example, to find the invariant density of the logistic map $f(x) = 4x(1 - x)$, we first find the preimages of the interval $[0, x]$. These can be easily found as

$$f^{-1}([0, x]) = \left[0, \frac{1}{2} - \frac{1}{2}\sqrt{1 - x}\right] \cup \left[\frac{1}{2} + \frac{1}{2}\sqrt{1 - x}, 1\right]$$

Equation (9) then becomes:

$$\begin{aligned} P\rho(x) &= \frac{d}{dx}\int_0^{1/2-1/2\sqrt{1-x}} \rho(y)dy \\ &\quad + \frac{d}{dx}\int_{1/2+1/2\sqrt{1-x}}^1 \rho(y)dy \end{aligned} \tag{10}$$

Leibniz's rule is used to evaluate the integrals in Eq. (10):

$$\frac{d}{dx}\int_{u(x)}^{v(x)} f(t)dt = f(v(x))\frac{dv}{dx} - f(u(x))\frac{du}{dx}$$

A simple calculation then gives us:

$$\begin{aligned} P\rho(x) &= \frac{1}{4\sqrt{1 - x}}\rho\left(\frac{1}{2} - \frac{1}{2}\sqrt{1 - x}\right) \\ &\quad + \rho\left(\frac{1}{2} + \frac{1}{2}\sqrt{1 - x}\right) \end{aligned} \tag{11}$$

Notice that this is a functional equation, and was famously solved by Ulam and von Neumann [1947].

$$\rho(x) = \frac{1}{\pi\sqrt{x(1 - x)}}$$

There is no general analytic method for solving such equations, although the invariant densities of some of the other well-known chaotic maps have been determined.

There is a useful alternative representation of the FPO for one-dimensional piecewise monotonic functions which is often cited in the literature. If we let $\chi_\sigma(y) = f_\sigma^{-1}(y)$ be the k preimages of y under f, with $\sigma = 1, \ldots, k$, then Eq. (6) can be written as:

$$\int_a^b \rho_{n+1}(x)dx = \sum_\sigma \int_{\chi_\square(a)}^{\chi_\square(b)} \rho_n(x)dx \tag{12}$$

In the right-hand integral, we make the substitution $x \to \chi_\sigma(y)$. We must find the derivative of $\chi_\sigma(y)$ by using the rule for derivatives of inverse functions:

$$\chi'_\sigma(y) = (f_\sigma^{-1})'(y) = \frac{1}{f'(f_\sigma^{-1}(y))} = \frac{1}{f'(\chi_\sigma(y))} \tag{13}$$

Equation (12) becomes

$$\int_a^b \rho_{n+1}(x)dx = \sum_\sigma \int_a^b \frac{\rho_n(\chi_\sigma(y))dy}{f'(\chi_\sigma(y))} \tag{14}$$

Since $f'(\chi_\sigma(y))$ is a constant and as $[a, b]$ is an arbitrary interval, the integrands on both sides must be equal, allowing us to write:

$$\rho_{n+1}(y) = \sum_\sigma \frac{\rho_n(\chi_\sigma(y))}{|f'(\chi_\sigma(y))|} \tag{15}$$

Finally, we rewrite Eq. (15) in operator form, and slightly simpler notation:

$$P\rho(y) = \sum_{x \in f^{-1}(y)} \frac{\rho(x)}{|f'(x)|} \tag{16}$$

Equation (16) can be used to give functional equations for the invariant densities of piecewise linear maps.

2.3. *The inverse Frobenius–Perron problem and the FPO as a Markov operator*

We saw in the previous section how the FPO gives rise to functional equations which must be solved for $\rho(x)$. This is a difficult (if not impossible) problem for arbitrary continuous maps: Firstly, the invariant density[1] may be a fractal or Cantor set, in which case the intervals concerned have measure zero[2]; secondly, it may not be possible to solve the resulting functional equations, assuming the invariant measure is continuous. So the inverse problem, of choosing an arbitrary invariant measure, and finding which map gives rise to it, must seem like quite an impossible task. All is not lost though. There are two main approaches to this inverse Frobenius–Perron problem (IFPP) in the literature. The first method uses a conjugate function approach, the second is based on approximation of the FPO by a Markov matrix.

The conjugate function approach, which was first described by Grossman and Thomae [1977], makes use of the following equivalence relation between two mappings: The maps $f : I \to I$ and $g : J \to J$ on intervals I and J are conjugate if there exists a one-to-one map $h : I \xrightarrow{\text{onto}} J$ such that

$$g(x) = h(f[h^{-1}(x)]) \tag{17}$$

The conjugating function h, assumed to be continuous and sufficiently smooth, establishes a one-to-one correspondence between the iterates of the two maps f and g. The invariant densities of g and h are related as follows:

$$\rho_g(x) = \rho_f[h^{-1}(x)] \left| \frac{dh^{-1}(x)}{dx} \right| \tag{18}$$

Numerous examples are given in the paper by Grossman and Thomae. Also, this approach can be used to find the invariant density of the logistic map. It is conjugate to the tent map through the conjugating function $h(x) = \sin^2(\pi x/2)$ (see [Ott, 2002] for details). The invariant density of the tent map is constant and equals one, and so Eq. (18) reduces to

$$\rho_g(x) = \left| \frac{dh^{-1}(x)}{dx} \right| \tag{19}$$

The inverse function h^{-1} can be shown as

$$h^{-1}(x) = \frac{2}{\pi} \sin^{-1}\sqrt{x} \tag{20}$$

We can find the derivative, and thus the required invariant density, as follows:

$$\rho_g(x) = \frac{d}{dx}\left(\frac{2}{\pi} \sin^{-1}\sqrt{x}\right) = \frac{1}{\pi\sqrt{x(1-x)}} \tag{21}$$

Figure 1 illustrates the two conjugate maps, the conjugating function $h(x) = \sin^2(\pi x/2)$, and the invariant densities of the logistic and tent maps.

The Markov matrix approach, upon which our new results are based, was first suggested by Ulam [1960]. The FPO is a Markov operator, in the sense that the density at step $n + 1$ is only a function of

[1] We assume that there is a single physically relevant invariant density, or natural invariant density [Ott, 2002], which is stable in the presence of weak random noise. There are infinitely many invariant densities, but they are not physically relevant [Schuster, 1989].

[2] The concept of sets of *measure zero* comes from Lebesgue integration, and means that they are negligible sets that can be ignored, as they can be enclosed within an arbitrarily small interval [Strichartz, 2000].

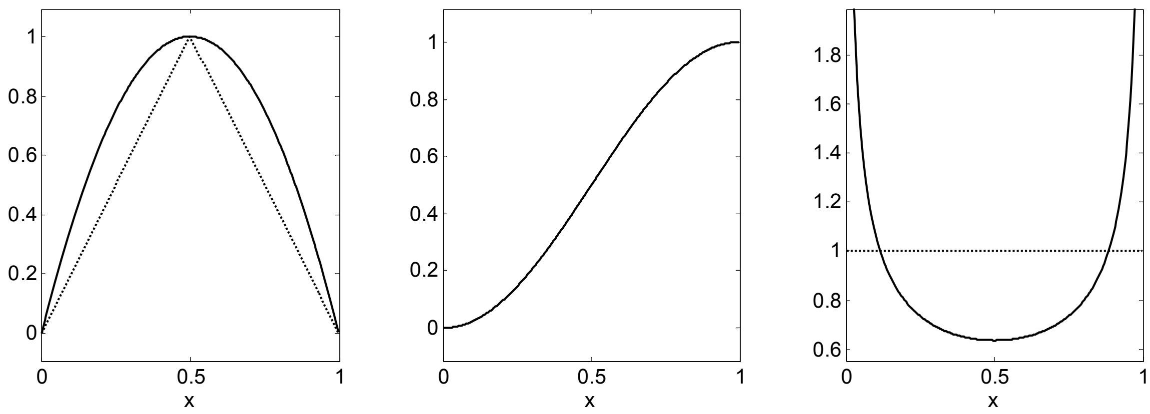

(a) (b) (c)

Fig. 1. (a) Logistic and tent maps, (b) Conjugating function, (c) Invariant densities of both maps.

the density at step n (see [Luenberger, 1979]). Ulam suggested that the state-space (the unit interval in all of our work) be arbitrarily partitioned into N subintervals, $I_1, \ldots, I_N$. Then define a probability vector at step n:

$$P_n = \left\{ \int_{I_1} \rho_n(x)dx, \ldots, \int_{I_N} \rho_n(x)dx \right\} \tag{22}$$

Now introduce an $N \times N$ transition matrix, W, which gives the probabilities of iterates moving from any subinterval to any other subinterval in the partition. Ulam hypothesized that the FPO could now be approximated by the following matrix equation:

$$P_{n+1} = WP_n \tag{23}$$

It is clear that as $N \to \infty$, Eq. (23) gives a better and better approximation of the FPO. Ulam's hypothesis was later proved by Li [1976]. It is remarkable that the statistical properties of chaotic systems can be represented by such a simple linear equation, allowing us to bring many of the results of positive matrix theory to bear on the problem.

2.4. *Other work on the IFPP and applications*

There has been a surprisingly large amount of work done on controlling the statistical properties of 1-D maps. Apart from the seminal work of Grossman and Thomae cited earlier, we mention the paper of Baranovsky and Daems [1995], in which piecewise linear Markov maps are used as references whose statistical properties are known. These maps are then transformed into non-Markov maps and smooth maps, using conjugating functions. They also consider the problem of designing maps with prescribed correlation functions.

Pingel, Schmelcher and Diakonos [Pingel *et al.*, 1999] manage to solve the Frobenius–Perron equation exactly for a class of unimodal chaotic maps, whose invariant densities are members of a class of beta distributions. By varying parameters in the maps which control symmetry and pointedness, they can obtain a variety of different invariant densities. Interestingly, the logistic map is a member of their class of maps. This group subsequently developed a Monte–Carlo approach, based on their class of parameterized maps, for generating maps with desired invariant densities and correlation functions [Diakonos *et al.*, 1999].

In a series of papers, the group led by Setti have studied the Markov approach to the IFPP with a view to applying it to signal processing tasks (see especially [Setti *et al.*, 2002] and the copious references therein). They consider a variety of piecewise linear maps including *n-way* Bernoulli shifts and develop a matrix-tensor formulation for quantifying high-order correlations of such maps. In [Setti *et al.*, 2002], they also discuss applying chaos to help with EMC (electromagnetic compatibility) issues, and they discuss the use of chaos in spread-spectrum communication schemes.

Another active area of research is the use of chaotic maps to model packet traffic in computer networks. Packet traffic is notoriously prone to bursts, and chaotic maps are ideal for modeling the fractal properties of the traffic. Mondragon neatly summarizes the previous work in this area in [Mondragon, 1999], and introduces some different types of intermittency maps along with a discussion of the statistical properties of these maps.

3. A Matrix Method for Solving the IFPP

A recent analysis of the Transmission Control Protocol (TCP) in synchronized communication networks [Shorten *et al.*, 2003; Berman *et al.*, 2004] gave rise to a positive matrix with special properties that allow us to solve the IFPP in an elegant way. In the TCP protocol, each data source is allocated a congestion window which governs how much data it can send. The protocol uses an Additive-Increase Multiplicative-Decrease (AIMD) algorithm for allocating window size: if the network is uncongested, the amount of data each source can send increases additively, but when congestion is detected, the sources back off in a multiplicative way [Tanenbaum, 2002]. It can be shown that if there are n sources competing for some finite bandwidth, and all these sources are operating the TCP congestion control algorithm in the presence of a drop-tail buffer bottleneck, then the dynamics of the system may be modeled by the following matrix equation:

$$W(k+1) = AW(k) \tag{24}$$

where $W(k)$ is a vector of the congestion windows of each source. The matrix A has the form:

$$A = \begin{pmatrix} \beta_1 & 0 & \cdots & 0 \\ 0 & \beta_2 & 0 & 0 \\ \vdots & 0 & \ddots & 0 \\ 0 & 0 & \cdots & \beta_n \end{pmatrix} + \frac{1}{\sum_{i=1}^{n} \alpha_i} \begin{pmatrix} \alpha_1 \\ \alpha_2 \\ \vdots \\ \alpha_n \end{pmatrix}$$
$$\times \begin{pmatrix} 1-\beta_1 & 1-\beta_2 & \cdots & 1-\beta_n \end{pmatrix} \tag{25}$$

The α_i are the additive increase parameters for each of the n sources, and the β_i are the corresponding multiplicative decrease parameters. The matrix A has many interesting properties which we outline here:

1. Matrix A is column stochastic (which means each column sums to 1).
2. The matrix is a positive matrix (all entries are positive real numbers).
3. The matrix has a single dominant eigenvalue of value 1.
4. There is a single eigenvector of A in the positive orthant called the Perron eigenvector, corresponding to the dominant eigenvalue, whose value is given by:
$$x_P^T = \left[\frac{\alpha_1}{1-\beta_1}, \frac{\alpha_2}{1-\beta_2}, \ldots, \frac{\alpha_n}{1-\beta_n}\right] \tag{26}$$
5. If the eigenvalues (λ_i) and the β_i are arranged in decreasing order, then the following interlacing scheme holds
$$1 = \lambda_1 > \beta_1 \geq \lambda_2 \geq \beta_2 \geq \cdots \geq \lambda_n \geq \beta_n \tag{27}$$

The interlacing result and the form of the Perron eigenvector are given in the paper by Wirth [Wirth *et al.*, 2006], and are based on standard results on the symmetric eigenvalue problem (see for example [Golub & van Loan, 1996], or [Horn & Johnson, 1985]).

We will be using the A matrix to describe the transition probabilities between intervals in a partition. At the heart of our synthesis approach is the Perron eigenvector of A: being parameterized in terms of the α_i and β_i unlocks the Inverse Frobenius–Perron Problem.

Ulam's conjecture was that the principle eigenvector of a Markov process is the invariant density of that process, and that transformations on the interval could be approximated using this matrix approach.

We have a way of choosing our invariant density first, and automatically determining a Markov process that gave rise to it. (Note that the Markov process is not unique.) The Markov process can then easily be turned into a chaotic map — in other words, a solution to the Inverse Ulam problem, as indicated by Bollt [2000].

3.1. *Synthesis procedure*

Suppose that the desired invariant density (Perron eigenvector) x_d is:

$$x_d^T = \rho = [\delta_1, \delta_2, \ldots, \delta_n] \tag{28}$$

Choose the β_i subject to the constraint: $0 < \beta_i < 1$, the β_i control depends on how rapidly the map converges on the invariant density (see [Rogers *et al.*, 2008]). Often, we find it convenient to keep all the β_i equal. Having chosen the β_i, determine the α_i as follows:

$$\alpha_1 = \delta_1(1-\beta_1)$$
$$\alpha_2 = \delta_2(1-\beta_2)$$
$$\vdots$$
$$\alpha_n = \delta_n(1-\beta_n)$$

Now form the matrix A from the α_i and β_i:

$$A = \begin{pmatrix} \beta_1 & 0 & \cdots & 0 \\ 0 & \beta_2 & 0 & 0 \\ \vdots & 0 & \ddots & 0 \\ 0 & 0 & \cdots & \beta_n \end{pmatrix} + \frac{1}{\sum_{i=1}^{n} \alpha_i} \begin{pmatrix} \alpha_1 \\ \alpha_2 \\ \vdots \\ \alpha_n \end{pmatrix} \times \begin{pmatrix} 1-\beta_1 & 1-\beta_2 & \cdots & 1-\beta_n \end{pmatrix}$$

Next, we let the A matrix represent a 1-D map on the unit interval to itself. We partition the unit interval into n equal subintervals, $\{I_1, \ldots, I_n\}$ (assuming A is an $n \times n$ matrix). Note that the partition can also be nonuniform. Let entry a_{ji} of A denote the probability of a transition from subinterval I_i to I_j. To construct the map, place a line segment of slope $\pm 1/a_{\text{ji}}$ in the square defined by the subintervals I_i, I_j, as illustrated in Fig. 2. By controlling the slope of the line segment, we can control how much of the overall subinterval will interact with that portion of the map, which in turn relates to the transition probabilities. In Fig. 2, the probability of a transition from I_1 to I_j is 0.5, corresponding to a line of slope 2 in that region. The rest of the chaotic map is constructed similarly.

3.2. *Example*

We now give an example of the synthesis procedure: Invariant density $x_d = \rho = [1, 2, 3]$. We let $\beta_i = 0.1$ for convenience. The values of α_i are computed to be $[0.9, 1.8, 2.7]$. The transition matrix A is then found to be:

$$A = \begin{pmatrix} 0.25 & 0.15 & 0.15 \\ 0.3 & 0.4 & 0.3 \\ 0.45 & 0.45 & 0.55 \end{pmatrix} \tag{29}$$

A is clearly column stochastic, and has eigenvalues of $[1, 0.1, 0.1]$, which we could have deduced from the interlacing property mentioned earlier. Figure 3 shows the one-dimensional map corresponding to matrix A and constructed in the manner outlined above. Figure 4 is the invariant density of the map after 20000 iterations. The y-axis has been scaled to allow a ready comparison with x_d. A typical chaotic time-series from the map is shown in Fig. 5.

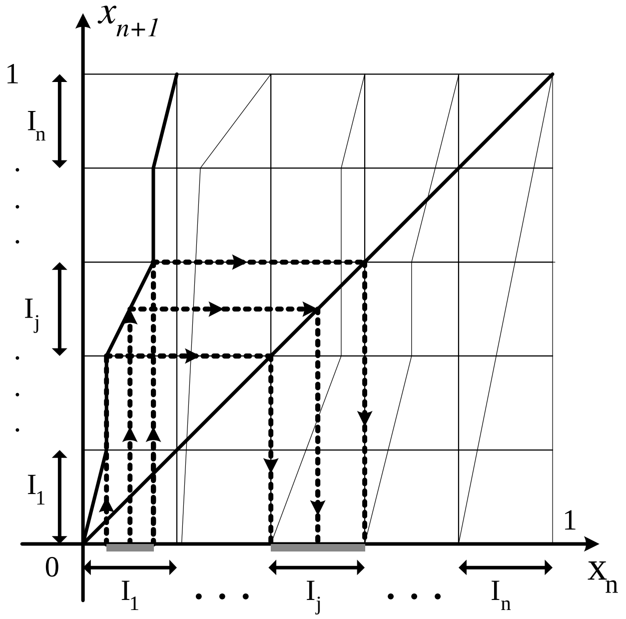

Fig. 2. Illustration of the construction of a 1-D map from a Markov matrix.

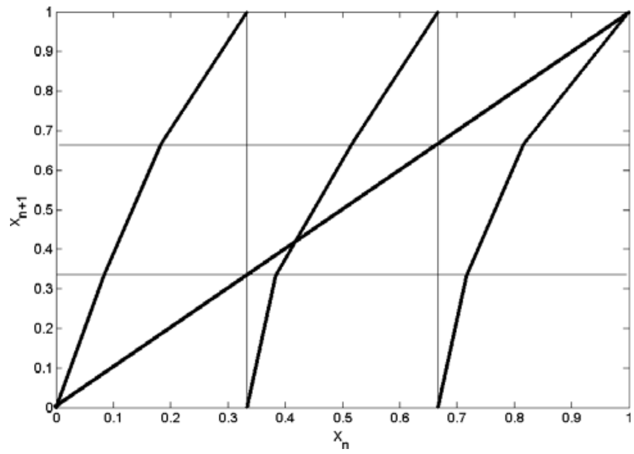

Fig. 3. One-dimensional chaotic map with partition on unit-interval shown.

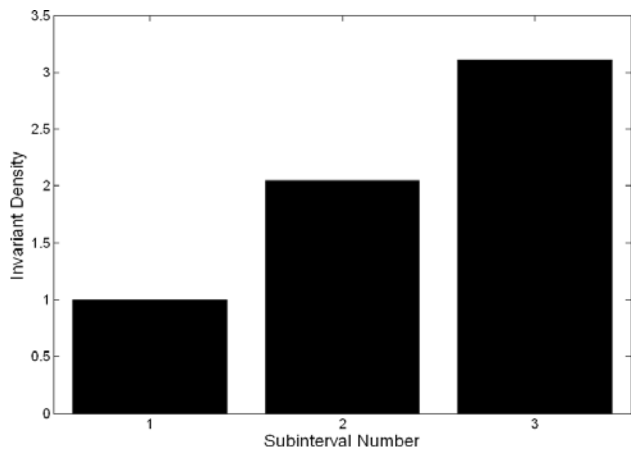

Fig. 4. Invariant density of map in Fig. 3.

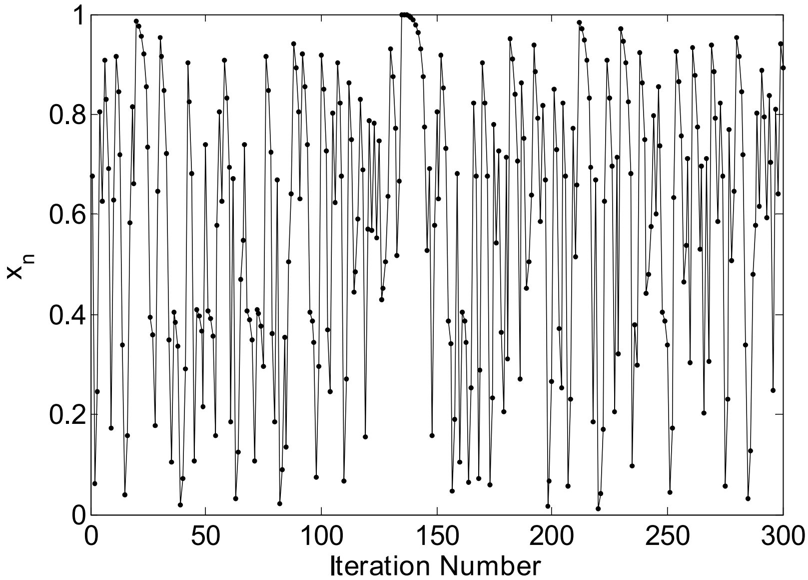

Fig. 5. Time-series of chaotic map in Fig. 3.

3.3. *Comparison with other methods*

As was mentioned earlier, there are several approaches to the IFPP described in the literature. They generally fall under three main headings:

1. Integration of the FPO
   Examples of this approach can be seen in the work of Pingel and the work of Kohda [Pingel *et al.*, 1999; Kohda, 2002]. Usually, the map and the density are assumed to have a certain form, or belong to a class of functions. For certain cases, such as unimodal maps, this yields closed form solutions to the Frobenius–Perron equation.
2. Conjugate-function approach
   In this approach, which was suggested by Ulam [1960], one tries to find a known invariant density (belonging to a known map) which can be conjugated (transformed via a simple function) to the desired invariant density. The required map can then be found via the conjugating function. This method is described in detail by Grossman and Thomae [1977].
3. Matrix-based approach
   These methods rely on the Ulam conjecture. Indeed, Bollt [2000] calls this approach to the IFPP the Inverse Ulam problem (IUP). The only approach which is directly comparable to ours is the method of Gora and Boyarsky. Their matrix method is outlined in their 1993 paper [Gora & Boyarsky, 1993] and more recently in their book [Boyarksy & Góra, 1997].

3.3.1. Three-band matrix solution to the IFPP

In [Gora & Boyarsky, 1993], the authors introduce a new class of piecewise linear transformation called a semi-Markov process, and a special matrix called a three-band matrix. They go on to prove a number of theorems around these new structures, showing that given some piecewise constant density on intervals of a partition, it is always possible to find a semi-Markov transformation that leaves the density invariant. We will show how they generate the three-band matrix, and then compare their method with our own using some examples.

Definition. A semi-Markov piecewise linear transformation, f, is a three-band transformation if its transition matrix $A = (a_{ij})$ satisfies: for any $1 \leq i \leq N$, $a_{ij} = 0$ if $|i - j| > 1$.

Theorem 3.1 [Gora & Boyarksy, 1993]. *Let f be a three-band transformation with transition matrix $A = (a_{ij})$. Let ρ be any f-invariant density and $\rho_i = \rho|_{R_i}$, $i = 1, \ldots, N$, then for $2 \leq i \leq N$ we have:*

$$a_{i,i-1} \cdot \rho_i = a_{i-1,i} \cdot \rho_{i-1} \tag{30}$$

A three-band matrix is one in which all the entries are zero except for the main diagonal entries and the entries adjacent to the main diagonal on either side. In terms of transitions between intervals on a partition, points may only be mapped to adjacent intervals, or stay in the same interval. The transition matrix is not symmetric in general.

Also, there exist infinitely many three-band transformations which preserve a given density function. This is in contrast to our method where the transition matrix is unique, given the α_i and β_i.

Equation (30) imposes a condition on the off-diagonal nonzero entries. Once this condition is satisfied, the rest of the entries may be chosen arbitrarily, ensuring that the matrix is column (or row) stochastic, of course.

Example. We will synthesize a chaotic map with the following invariant density: $\rho = (5/16)(1,8,4,2,1)$ first using the three-band approach, and then using our approach. Applying Eq. (30), we get the following conditions:

$$\frac{40}{16}a_{21} = \frac{5}{16}a_{12} \Rightarrow 8a_{21} = a_{12}$$
$$\frac{20}{16}a_{32} = \frac{40}{16}a_{23} \Rightarrow a_{32} = 2a_{23}$$
$$\frac{10}{16}a_{43} = \frac{20}{16}a_{34} \Rightarrow a_{43} = 2a_{34}$$
$$\frac{5}{16}a_{54} = \frac{10}{16}a_{45} \Rightarrow a_{54} = 2a_{45}$$

Now we arbitrarily choose the entries as follows: $a_{21} = 0.1 \Rightarrow a_{12} = 0.8$, $a_{32} = 0.4 \Rightarrow a_{23} = 0.2$, $a_{43} = 0.4 \Rightarrow a_{34} = 0.2$, $a_{54} = 0.8 \Rightarrow a_{45} = 0.4$. The transition matrix now looks like:

$$A = \begin{pmatrix} & 0.8 & 0 & 0 & 0 \\ 0.1 & & 0.2 & 0 & 0 \\ 0 & 0.4 & & 0.2 & 0 \\ 0 & 0 & 0.4 & & 0.4 \\ 0 & 0 & 0 & 0.8 & \end{pmatrix}$$

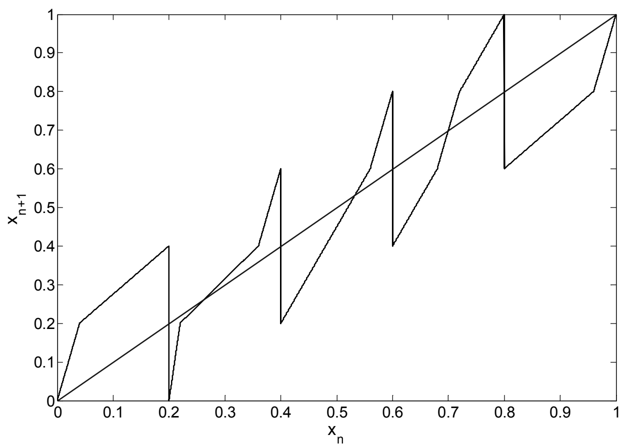

Fig. 6. Chaotic map synthesized using the matrix method of Gora and Boyarsky.

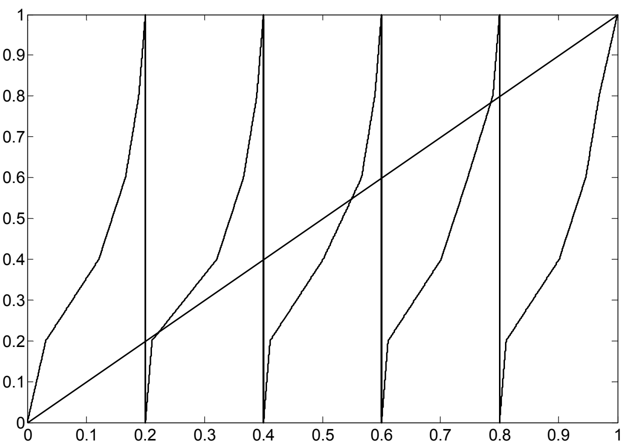

Fig. 7. Chaotic map with same invariant density as that in Fig. 6.

Next, we fill in the gaps, ensuring the matrix is row stochastic, to get:

$$A = \begin{pmatrix} 0.2 & 0.8 & 0 & 0 & 0 \\ 0.1 & 0.7 & 0.2 & 0 & 0 \\ 0 & 0.4 & 0.4 & 0.2 & 0 \\ 0 & 0 & 0.4 & 0.2 & 0.4 \\ 0 & 0 & 0 & 0.8 & 0.2 \end{pmatrix}$$

Matrix A has the following eigenvalues: $[1.0, 0.786, 0.31, 0.031, -0.42]$, and its dominant eigenvector corresponds to the desired invariant density. The chaotic map arising from A is shown in Fig. 6, and a chaotic map generated using our procedure (using $\beta_i = 0.1$) is shown in Fig. 7. It is extraordinary that different chaotic maps give rise to the same invariant density. Indeed, there are an infinite number of possible maps, based both on our method, and that of Gora and Boyarsky, that would give the same density. The main disadvantage of their method is that there are $N - 1$ independent parameters that must be chosen. In [Gora & Boyarsky, 1993], the authors do mention that additional criteria (such as Lyapunov exponents) need to be used to ensure the map is unique.

4. Autocorrelation Properties

Apart from the invariant density, another key statistical property of chaotic maps is autocorrelation, which can be thought of as a measure of how quickly two nearby trajectories diverge. In this work, it is also related to how quickly the invariant density is approached. The autocorrelation function of a chaotic map decays from one down to zero because of sensitivity to initial conditions. In the maps we have been studying, the autocorrelation function is heavily dependent on the value of the β_i parameters. For large values of β_i the diagonal values of A are approximately equal to β_i, and the off-diagonal entries are close to zero because of the $1-\beta_i$ terms in Eq. (25). The slopes of the segments in the map are thus close to 1, and nearby trajectories diverge slowly. The autocorrelation function decays slowly to zero in this case. If β_i are close to zero, then the A matrix is dominated by α_i terms. The values of the slopes tend to be large, and nearby trajectories diverge rapidly, leading to a rapid decay of the autocorrelation function (see Fig. 8). It is clearly of interest that in synthesizing chaos we have this second degree of freedom, apart from the invariant density itself.

The autocorrelation function $R(\tau)$ is defined as [Box *et al.*, 1994]:

$$R(\tau) = \frac{C(\tau)}{C(0)} \tag{31}$$

where

$$\begin{aligned} C(\tau) &= \frac{1}{M}\sum_{i=1}^{M-\tau}(x_i-\overline{x})(x_{i+\tau}-\overline{x}) \\ &= \frac{1}{M}\sum_{i=1}^{M-\tau}(x_i-\overline{x})(f^{(\tau)}(x_i)-\overline{x}) \end{aligned} \tag{32}$$

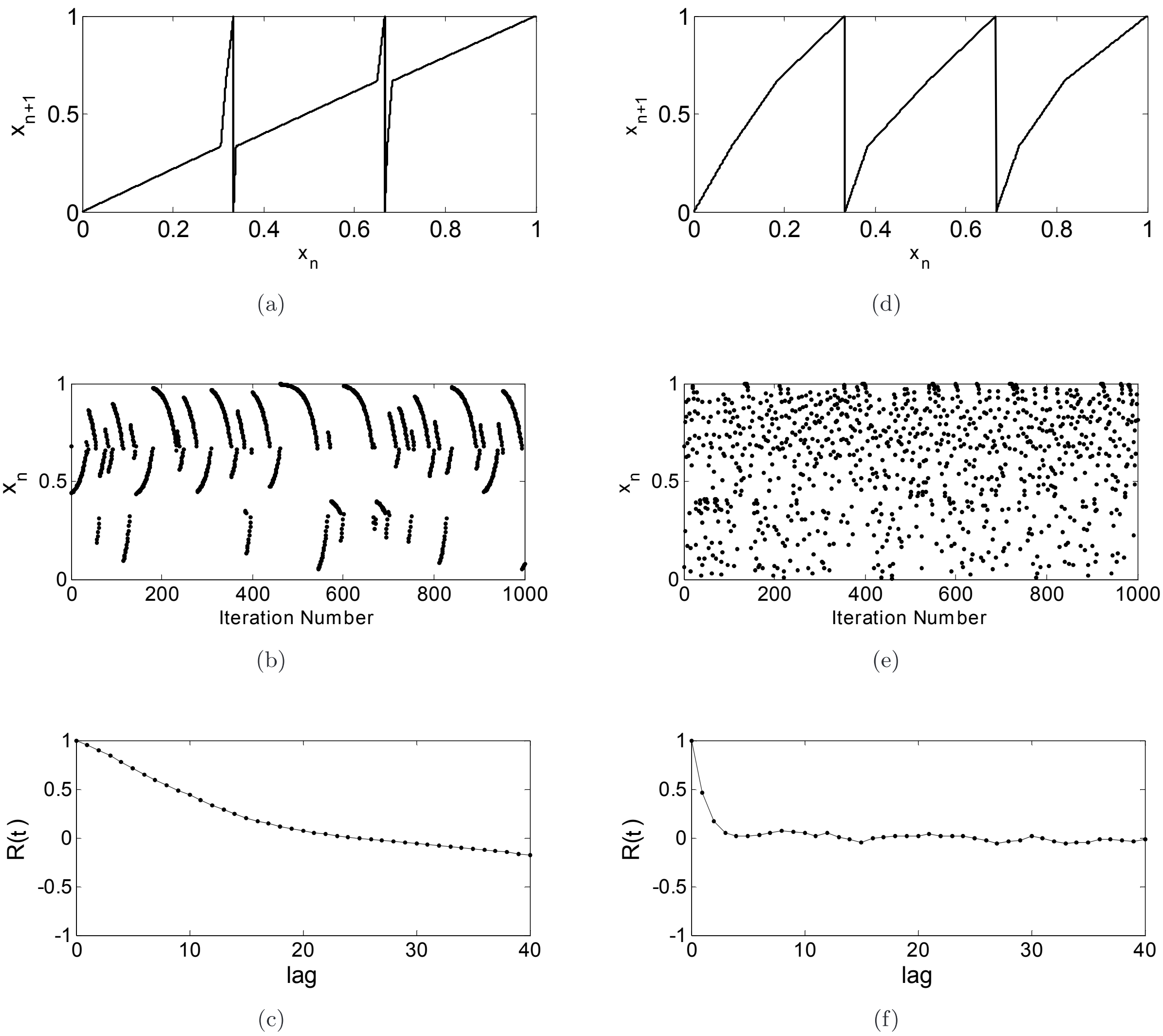

Fig. 8. (a)–(c) 1-D map, time-series and autocorrelation plots with □i = 0:9; (d)–(f) □i = 0:1. Both maps have the same invariant density □= [1; 2; 3].

and $C(0)$ is the variance

$$C(0) = \sigma^2 = \frac{1}{M}\sum_{i=1}^{M}(x_i - \overline{x})^2 \tag{33}$$

Note that $f^{(\tau)}$ denotes τ-times composition of the map f, and M is the number of points in the time-series.

These equations may be used to determine the autocorrelation from the chaotic time-series. It is also possible to use the Markov property of the map to write down an expression in terms of the map parameters and transition matrix elements:

$$E[x_n x_{n-\tau}] = \sum_{j=1}^{N}\sum_{k=1}^{N} x(k)x(j)\,p_j\,p_{jk}(\tau) \tag{34}$$

where

$x(j)$ is the value of state j
$x(k)$ is the value of state k
p_j is the probability of being in state j
p_{jk} is the probability of moving from state j to state k in τ time-steps
N is the number of states in the Markov chain.

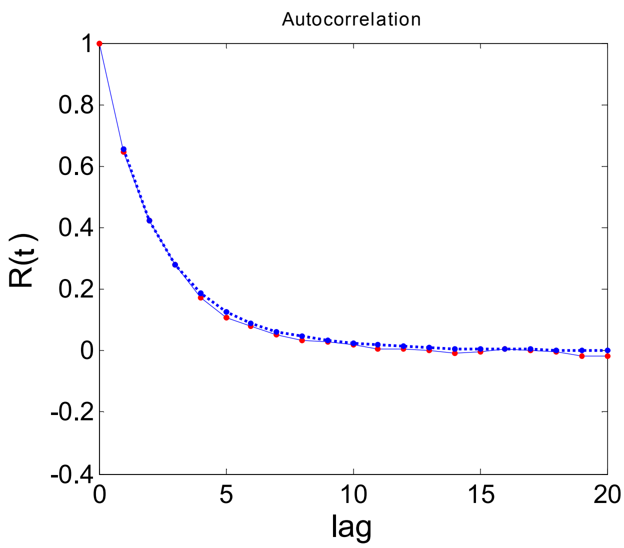

Fig. 9. Actual and theoretical (dotted line) autocorrelation values for a 20×20 transition matrix/map.

We also have that

$$p_{jk}(\tau) = \sum_{n=1}^{N} p_{jn}\,p_{nk}(\tau - 1) = (A^\tau)_{jk} \tag{35}$$

The x variable can take on any value within a subinterval (state), but as the invariant densities

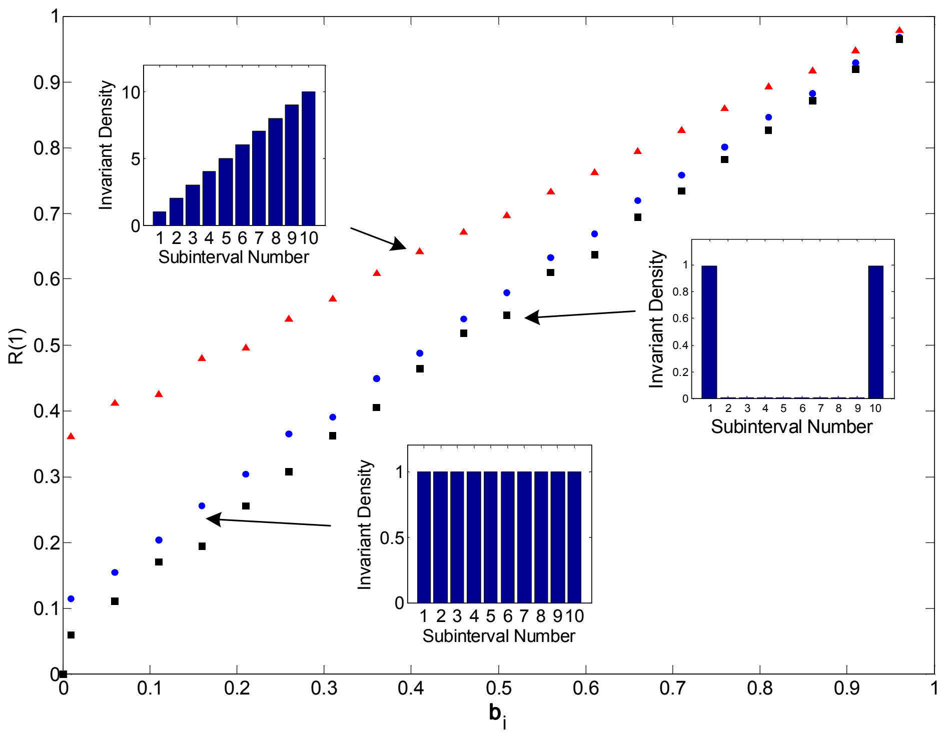

Fig. 10. Lag-1 autocorrelation coefficient variation against $\square_i$ for three different invariant densities.

are constant within a subinterval, the midpoint of each subinterval can be taken as the value of x. The expression for the autocorrelation is then

$$R(\tau) = \frac{1}{\sigma^2}\sum_{j=1}^{N}\sum_{k=1}^{N}\left(\frac{j}{N} - \frac{1}{2N}\right)\left(\frac{k}{N} - \frac{1}{2N}\right) \times \frac{\alpha_j}{1-\beta j}(A^\tau)_{jk} - \overline{x}^2 \tag{36}$$

where

$$\overline{x}^2 = \sum_{i=1}^{N} \frac{\alpha_i}{1-\beta_i}\cdot\frac{2i-1}{2N} \tag{37}$$

Here we have assumed that the trajectory is ergodic and so the time-average and space-average of x are equal, and that the choice of initial condition is almost always unimportant. Clearly Eq. (36) is an approximation but it becomes very close to the real autocorrelation as N gets large. Figure 9 shows a typical autocorrelation curve from a chaotic time-series generated from a 20×20 transition matrix, along with the predicted value using Eq. (36).

The values of the correlation coefficients appear to increase linearly with β_i as illustrated in Fig. 10. Here we show variation in the lag-1 autocorrelation coefficient $C(1)$ against β_i for three different invariant distributions. Note that we vary all of the β_i from 0 to 1 in the graph. The constant invariant density (lower left inset) and the twin-peak density (lower right inset) have much lower values of autocorrelation coefficient compared with the ramp-type invariant density (upper left inset). It may be possible to model the effect of the β_i on the correlation coefficients, and this will be the focus of future work.

5. Switching Between Chaotic Maps

An interesting extension of the work in Sec. 3 is to consider what happens when we switch randomly between some set of 1-D maps at each iteration of the process. This question has been considered by Boyarsky and Gora [2002], where they use this process to model the famous two-slit experiment in quantum physics. In the work below, each chaotic map's invariant density acts like a basis vector, and the overall invariant density of the switched system is a linear combination of the basis invariant densities.

Theorem 5.1. *Let $A(k) \in A_1, A_2$ and let $p_k = p(A(k))$ be chosen from the set. Assume the values of β_i to be the same for both maps. Let ρ_1 and ρ_2 be the invariant densities of the two maps. If we choose either A_1 or A_2 randomly (identically distributed independently) at each step of an iterative process with fixed probabilities p_1 and p_2 respectively, then the invariant density of the resultant orbit, ρ is given by $\rho = p_1\rho_1 + p_2\rho_2$.*

Proof.

$$A_1 = \begin{pmatrix} \beta_1 & 0 & \cdots & 0 \\ 0 & \beta_2 & 0 & 0 \\ \vdots & 0 & \ddots & 0 \\ 0 & 0 & \cdots & \beta_n \end{pmatrix} + \begin{pmatrix} \alpha_1 \\ \alpha_2 \\ \vdots \\ \alpha_n \end{pmatrix} \times \begin{pmatrix} 1-\beta_1 & 1-\beta_2 & \cdots & 1-\beta_n \end{pmatrix}$$

$$A_2 = \begin{pmatrix} \beta_1 & 0 & \cdots & 0 \\ 0 & \beta_2 & 0 & 0 \\ \vdots & 0 & \ddots & 0 \\ 0 & 0 & \cdots & \beta_n \end{pmatrix} + \begin{pmatrix} \hat{\alpha}_1 \\ \hat{\alpha}_2 \\ \vdots \\ \hat{\alpha}_n \end{pmatrix} \times \begin{pmatrix} 1-\beta_1 & 1-\beta_2 & \cdots & 1-\beta_n \end{pmatrix}$$

It is well known that the expected value of the transition matrix which results when switching randomly between two matrices is given by $A_0 = E(\Pi_k) = p_1A_1 + p_2A_2$.

By simple substitution we can show that

$$A_0 = \begin{pmatrix} \beta_1 & 0 & \cdots & 0 \\ 0 & \beta_2 & 0 & 0 \\ \vdots & 0 & \ddots & 0 \\ 0 & 0 & \cdots & \beta_n \end{pmatrix} + \begin{pmatrix} p_1\alpha_1 + p_2\hat{\alpha}_1 \\ p_1\alpha_2 + p_2\hat{\alpha}_2 \\ \vdots \\ p_1\alpha_n + p_2\hat{\alpha}_n \end{pmatrix} \times \begin{pmatrix} 1-\beta_1 & 1-\beta_2 & \cdots & 1-\beta_n \end{pmatrix}$$

A_0 thus has a Perron eigenvector of

$$x_P^T = \left[\frac{p_1\alpha_1 + p_2\hat{\alpha}_1}{1-\beta_1}, \frac{p_1\alpha_2 + p_2\hat{\alpha}_2}{1-\beta_2}, \ldots, \frac{p_1\alpha_n + p_2\hat{\alpha}_n}{1-\beta_n}\right] \tag{38}$$

□

Theorem 3.1 shows that when the values of β are the same in each matrix, the overall invariant density is just a weighted sum of the invariant densities of the original maps. This result also holds when switching between any number of maps. We illustrate this in the figures below where we switch

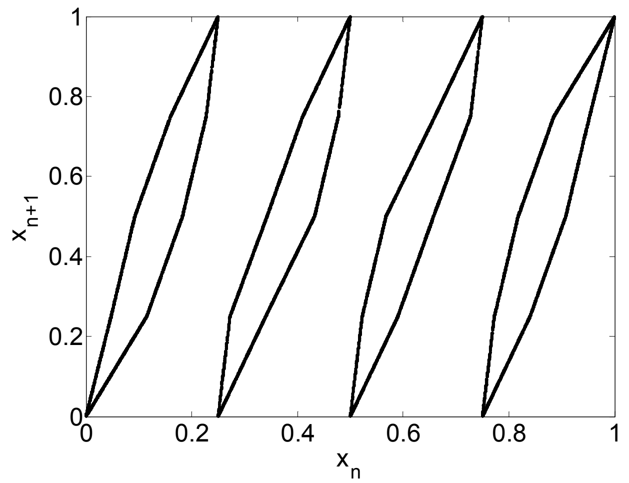

Fig. 11. State-space plot of switched-chaotic map.

between two maps. The maps have invariant densities $\rho_1 = 0.1[1, 2, 3, 4]$ and $\rho_2 = 0.1[4, 3, 2, 1]$, and each map is chosen with probability 0.5. As can be seen in Fig. 11 the state-space plot of the switched system is just the superposition of the two individual maps, and the invariant density shown in Fig. 12 is the average of the two individual invariant densities.

We now look at a more general case where the values of β_i are not necessarily the same in each matrix.

Theorem 5.2. *Let $A(k) \in A_1, A_2, \ldots, A_m$ and let $p_k = p(A(k))$ be chosen from the set. Let $\Pi_k = A(k)A(k-1)\cdots A(1)$. If $A(k)$ represents a chaotic map, then the expected invariant density obtained by switching randomly between the $A(k)$ is given by the Perron eigenvector of the following matrix: $B = p_1A_1 + p_2A_2 + \cdots + p_mA_m$.*

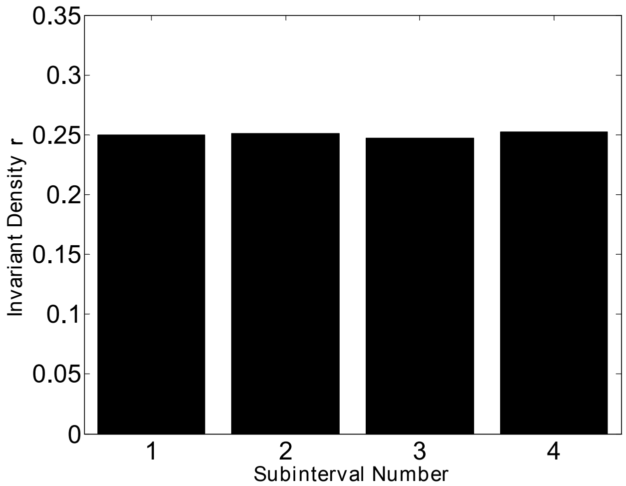

Fig. 12. Invariant density of switched chaotic map: average of constituent invariant densities.

Proof. The expected value, $E(\Pi_k) = (p_1A_1 + p_2A_2 + \cdots + p_mA_m)^k = B^k$ for any k. Given a stochastic matrix P, there exists a unique probability vector $\hat{p} > 0$ such that $P\hat{p} = \hat{p}$. Let x_0 be some initial condition. We then have that the eigenvector

$$\hat{p} = \lim_{k\to\infty} P^k x_0 \tag{39}$$

If P represents a map, then $\hat{p}$ is the invariant density of that map (Ulam's conjecture). As long as B is a stochastic matrix (easy to show), the result follows. □

Unfortunately, Theorem 4.2 does not give us a closed form expression for the expected invariant density, though it is possible to obtain expressions when the number and dimension of the matrices are small.

1. **Switching between two 2×2 matrices**
   As before, we let the probability of choosing A_1 be p_1 and that of choosing A_2 be p_2, where $p_1 + p_2 = 1$. It is assumed that the values of β_i are different for both matrices. The expected value of the overall transition matrix resulting from the switching is:

$$\begin{aligned} B &= p_1A_1 + p_2A_2 \\ &= p_1\left[\begin{pmatrix}\beta_1 & 0\\ 0 & \beta_2\end{pmatrix} + \begin{pmatrix}\alpha_1\\ \alpha_2\end{pmatrix}\begin{pmatrix}1-\beta_1 & 1-\beta_2\end{pmatrix}\right] \\ &\quad + p_2\left[\begin{pmatrix}\overline{\beta}_1 & 0\\ 0 & \overline{\beta}_2\end{pmatrix} + \begin{pmatrix}\overline{\alpha}_1\\ \overline{\alpha}_2\end{pmatrix}\begin{pmatrix}1-\overline{\beta}_1 & 1-\overline{\beta}_2\end{pmatrix}\right] \end{aligned}$$

   To find the Perron eigenvector $(x, y)^T$, we solve the following matrix equation, where the terms $a \cdots d$ represent the complicated expressions when the above equation is multiplied out:

$$\begin{pmatrix}a & b\\ c & d\end{pmatrix}\begin{pmatrix}x\\ y\end{pmatrix} = \begin{pmatrix}x\\ y\end{pmatrix} \tag{40}$$

   Solving Eq. (40), arbitrarily assuming $y = 1$, we find that the Perron eigenvector has the following form:

$$\begin{pmatrix}x\\ y\end{pmatrix} = \begin{pmatrix}\dfrac{p_1\alpha_1(1-\beta_2) + p_2\overline{\alpha}_1(1-\overline{\beta}_2)}{p_1\alpha_2(1-\beta_1) + p_2\overline{\alpha}_2(1-\overline{\beta}_1)]}\\ 1\end{pmatrix} \tag{41}$$

2. **Switching between three 2 □ 2 matrices**
If we have three matrices A_1, A_2, A_3 with associated probabilities p_1, p_2 and p_3, it is straightforward to show that the Perron eigenvector is as follows, again assuming that $y = 1$:

$$\begin{pmatrix} x \\ y \end{pmatrix} = \begin{pmatrix} \dfrac{p_1\alpha_1(1-\beta_2) + p_2\hat{\alpha}_1(1-\hat{\beta}_2) + p_3\overline{\alpha}_1(1-\overline{\beta}_2)}{p_1\alpha_2(1-\beta_1) + p_2\hat{\alpha}_2(1-\hat{\beta}_1) + p_3\overline{\alpha}_2(1-\overline{\beta}_1)} \\ 1 \end{pmatrix} \tag{42}$$

Comparing this with Eq. (41), a pattern emerges, allowing us to write down a general expression for switching between N different 2×2 matrices:

$$\begin{pmatrix} x \\ y \end{pmatrix} = \begin{pmatrix} \dfrac{\displaystyle\sum_{i=1}^{N} p_i\alpha_{1i}(1-\beta_{2i})}{\displaystyle\sum_{i=1}^{N} p_i\alpha_{2i}(1-\beta_{1i})} \\ 1 \end{pmatrix} \tag{43}$$

3. **Switching between two 3 □ 3 matrices**
As the matrices get bigger, the calculations become more laborious. For the 3×3 case, we find the Perron eigenvector $(x, y, z)^T$ to have the following form:

$$\begin{pmatrix} x \\ y \\ z \end{pmatrix} = \begin{pmatrix} \dfrac{p_1^2\alpha_1(1-\beta)^2 + p_2^2\hat{\alpha}_1(1-\hat{\beta})^2 + p_1p_2(1-\beta)(1-\hat{\beta})(\alpha_1+\hat{\alpha}_1)}{p_1^2\alpha_3(1-\beta)^2 + p_2^2\hat{\alpha}_3(1-\hat{\beta})^2 + p_1p_2(1-\beta)(1-\hat{\beta})(\alpha_3+\hat{\alpha}_3)} \\ \dfrac{p_1^2\alpha_2(1-\beta)^2 + p_2^2\hat{\alpha}_2(1-\hat{\beta})^2 + p_1p_2(1-\beta)(1-\hat{\beta})(\alpha_2+\hat{\alpha}_2)}{p_1^2\alpha_3(1-\beta)^2 + p_2^2\hat{\alpha}_3(1-\hat{\beta})^2 + p_1p_2(1-\beta)(1-\hat{\beta})(\alpha_3+\hat{\alpha}_3)} \\ 1 \end{pmatrix} \tag{44}$$

Here, we have assumed $z = 1$ to fix the vector, and we have also assumed $\beta_1 = \beta_2 = \beta_3 = \beta$ for matrix A_1, and for matrix A_2 all of the β values are equal to $\hat{\beta}$. There is a pleasing symmetry to the expressions, although we have not been able to write it in a simpler form.

Another interesting case is what is the resulting invariant density when we switch periodically between two of the synthesized chaotic maps. It turns out that it does not matter what order the maps are iterated in, periodic switching and random switching lead to the same result. We outline the proof here.

Theorem 5.3. *Let A_1 and A_2 be two transition matrices with corresponding chaotic maps f_1 and f_2. Let the transition matrices be rank 1 matrices (or close to rank 1 matrices), e.g. $\beta_i \to 0$. Let f_1 and f_2 possess invariant densities of ρ_1 and ρ_2, respectively. Suppose we iterate, switching periodically between maps f_1 and f_2. If t_1 and t_2 are the fractions of time spent iterating maps f_1 and f_2, respectively, then the resultant invariant density is given by $\rho = t_1\rho_1 + t_2\rho_2$.*

Outline Proof. We consider two different situations. First, iterate map f_1 N times, and then iterate map f_2 N times, so that the overall period is $2N$. Starting from an initial condition x_0, we have:

$$x_0 \to f_1(x_0) \to f_1^{(2)}(x_0) \to \cdots \to f_1^{(N)}(x_0)$$

N iterates will approach the invariant density ρ_1 asymptotically for large N, by definition. Now switch to map f_2 and iterate for N iterations:

$$f_1^{(N)}(x_0) = x_0' \to f_1(x_0') \to f_1^{(2)}(x_0') \to \cdots \\ \to f_1^{(N)}(x_0')$$

The N iterates of f_2 will approach the invariant density ρ_2, but considering all $2N$ iterates together, the invariant density is $\rho = (\rho_1 + \rho_2)/2$. This is clearly true for large N but what happens if N is small?

Let $N = 1$, and consider the iterates of f_1 as supplying initial conditions for f_2 and vice versa. An ensemble of initial conditions, when mapped under f_1, will have an invariant density ρ_1, and similarly f_2 will have an invariant density ρ_2. The initial conditions will not be uniformly distributed across the interval $[0, 1]$, but will be piecewise constant across the subintervals of the Markov partition. (It is a standard result that piecewise affine maps have piecewise constant invariant densities.) In rank 1 matrices all columns are equal, and thus the slopes in each subinterval are the same. It makes no difference which subinterval the initial conditions are in, so long as they are uniformly distributed in that subinterval (see Fig. 13). So, switching with $N = 1$ for, say, M periods, will lead to the ensemble of M initial conditions from map f_1 being mapped under f_2 resulting in an invariant density ρ_2, and similarly the other M initial conditions will result in an invariant density ρ_1. Taking all $2M$ iterates together, the invariant density is, once again, $\rho = (\rho_1 + \rho_2)/2$. □

Clearly, this result holds for any type of periodic sequence between any number of maps, so long as they are rank 1 matrices (or close to rank 1 matrices). The result also implies that periodic switching is just a special case of random switching for these types of maps.

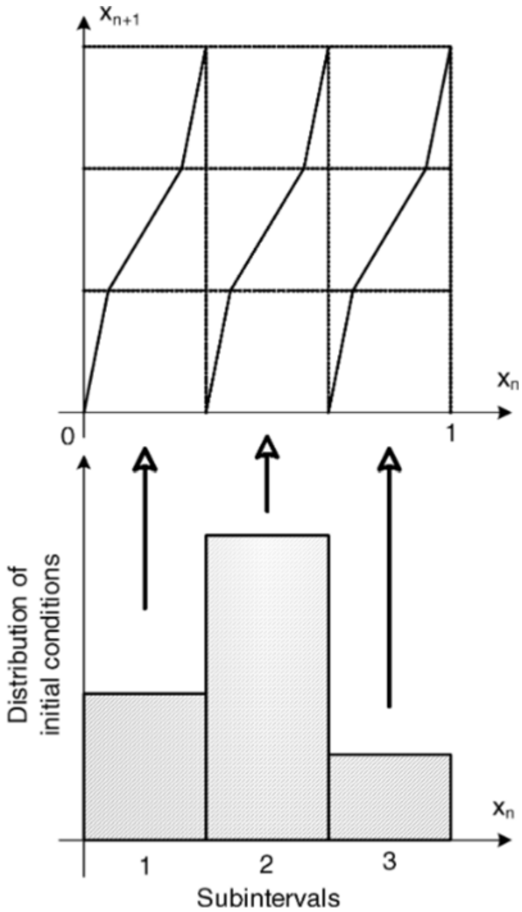

Fig. 13. Piecewise constant distribution of initial conditions being applied to chaotic map derived from a rank 1 transition matrix.

6. Applications to Image Generation

We have shown how to synthesize one-dimensional maps using the method based on positive matrix theory, and now wish to extend this method to two-dimensional maps, and possibly to N-dimensional maps. We describe two possible ways of doing this. The first method shown below generates a pseudo two-dimensional chaotic map from a one-dimensional map. A second method is given by Bollt [2000] and is based on affine functions. These methods are easily extendable to higher-dimensions. We then show how an image can be embedded within the invariant density of a 2-D map, so that the iteration of the map gradually reveals the picture.

6.1. *Pseudo 2-D map from 1-D map*

We start by partitioning the unit square into N^2 smaller squares each of side $1/N$. We then number the squares consecutively from 1 to N^2, and arrange the squares in a line, and then rescale the squares so that they are all contained in the unit interval. We form a 1-D vector of the desired densities, and use the synthesis method to form a transition matrix, as outlined elsewhere. The transition matrix is transformed into a 1-D chaotic map, producing some sequence of iterates p_n. We generate the 2-D map essentially by transforming this 1-D time series into our required form, by mapping each iterate to a point in the unit square. The x_n iterates are produced from the p_n using a simple modulo operation. We generate the y_n iterates by performing a Bernoulli shift on each p_n iterate. This ensures that the sequence of y iterates is also chaotic. The transformations required are:

$$x_n = Np_n \mod 1 \tag{45}$$

$$y_n = \frac{kp_n - \lfloor kp_n \rfloor + \lfloor Np_n \rfloor}{N}, \quad k \gg 1 \tag{46}$$

6.2. *N-dimensional maps*

Clearly this method is easily extendable to N-dimensional maps. For the 3-D case, we partition the unit cube into N^3 smaller cubes, and form a one-dimensional vector of desired densities in each little cube. We then work backwards, this time applying

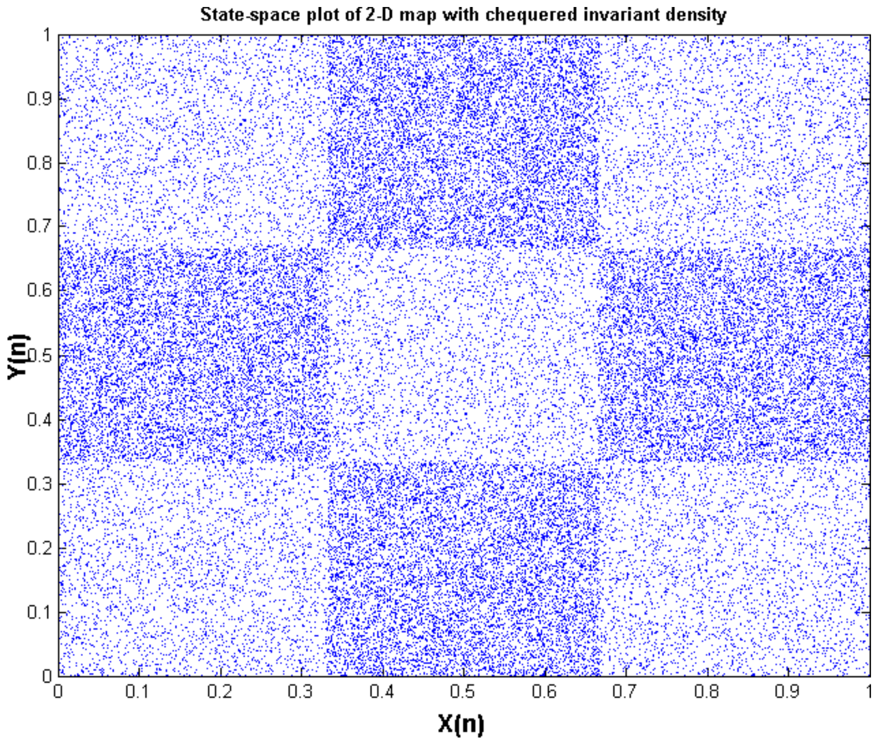

Fig. 14. Synthesized 2-D map with chequer-board invariant density.

two Bernoulli shifts to each chaotic iterate to generate a three-dimensional chaotic trajectory.

6.3. *Bollt's affine function method*

In [Bollt, 2000], the author introduces piecewise affine transformations $f_n : Q \to Q$, $Q \in \Re^2$, where the Q_i form a grid, which have similar properties to Anosov diffeomorphisms in that they have expanding and contracting directions and are invertible. The transformation is designed to have the column stochastic matrix A as its Frobenius–Perron operator. In his paper, Bollt uses control theory methods to achieve a desired invariant density. We shall apply our new synthesis method to generate the transition matrix, and then use Bollt's affine functions to realize the chaotic map. The construction of the affine functions is illustrated in Fig. 16. Following Bollt's notation, we partition the unit square into a grid of sub-squares Q_i each of side ϵ. The transition matrix A then determines the proportion of each Q_i that maps to another cell Q_j. The rule used is that $100 \cdot A_{\mathrm{ji}}\%$ of cell Q_i is mapped onto $100 \cdot A_{\mathrm{ji}}/\sum_k A_{jk}\%$ of Q_j. Horizontal strips of the cell Q_i are compressed in the x-direction, and expanded in the y-direction using the affine transformation:

$$\mathbf{f}_n^{\mathrm{ij}}(x,y) = \begin{pmatrix} f_n^{\mathrm{ij}}(x) \\ g_n^{\mathrm{ij}}(y) \end{pmatrix} = \begin{pmatrix} \dfrac{\Delta x'_{\mathrm{ji}}}{\Delta x_{\mathrm{ji}}} & 0 \\ 0 & \dfrac{\Delta y'_{\mathrm{ji}}}{\Delta y_{\mathrm{ji}}} \end{pmatrix} \cdot \begin{pmatrix} x - x_{\mathrm{ji}} \\ y - y_{\mathrm{ji}} \end{pmatrix} + \begin{pmatrix} x'_{\mathrm{ji}} \\ y'_{\mathrm{ji}} \end{pmatrix} \tag{47}$$

Equation (47) takes the rectangle $R_{\mathrm{ji}} = \Delta x_{\mathrm{ji}} \times \Delta y_{\mathrm{ji}}$ (as shown in Fig. 16) and maps it onto the rectangle $R'_{\mathrm{ji}} = \Delta x'_{\mathrm{ji}} \times \Delta y'_{\mathrm{ji}}$. In our implementation, we mapped rectangles progressively starting from the lower edge of Q_i onto the left edge of Q_j, though there are other possibilities.

The action of the map 47 is similar to the action of the Baker's map, leading to striations along the y-direction. There is also self-similarity evident in the density of orbits in each partition element, which arises naturally from the action of the map, as illustrated in Fig. 15.

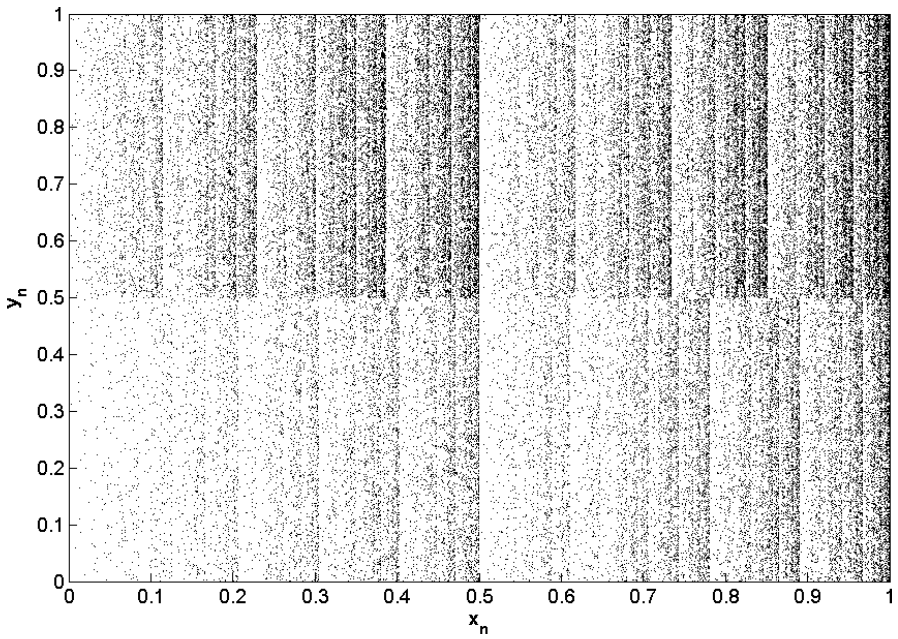

Fig. 15. Iterates of a synthesized map with □ = 1; 2; 3; 4 showing self-similar structure.

Bollt mentions several lemmas relating to the transformation $\mathbf{f}_n$, including that the transformation is hyperbolic if the transition matrix A is irreducible and aperiodic, and that the grid does indeed form a Markov partition under these circumstances.

6.4. *Statistical image generation*

An interesting application of 2-D map synthesis is that one can generate maps which, upon iteration, will generate a desired pattern, image or code. The image or code only appears after many thousands of iterations. As an example, we will encode part of the well-known *Lena* image in a 2-D chaotic map, and then observe how the image emerges upon iteration of the map.

We have taken a small section of the original image (30 × 30 pixels) in order to keep the transition matrix of a manageable size. The image is a matrix of numbers ranging from 1 to 128 representing gray-scales from black to white. We converted this matrix to a 900×1 vector representing the invariant density of a one-dimensional map, using the synthesis method presented in Sec. 3. We then synthesized the required 900 × 900 transition matrix which would give rise to this invariant density (using $\beta_i = 0.1$). This matrix was then

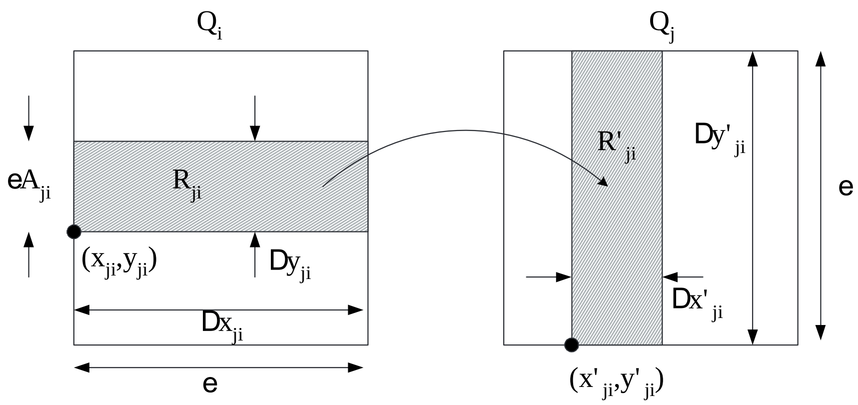

Fig. 16. Bollt's piecewise affine function designed as an Anosov diffeomorphism.

Fig. 17. Steps involved in encoding an image.

used to generate a set of affine functions according to Bollt's method, and these functions were iterated from some random initial condition in the unit square. The procedure is synopsized in Fig. 17.

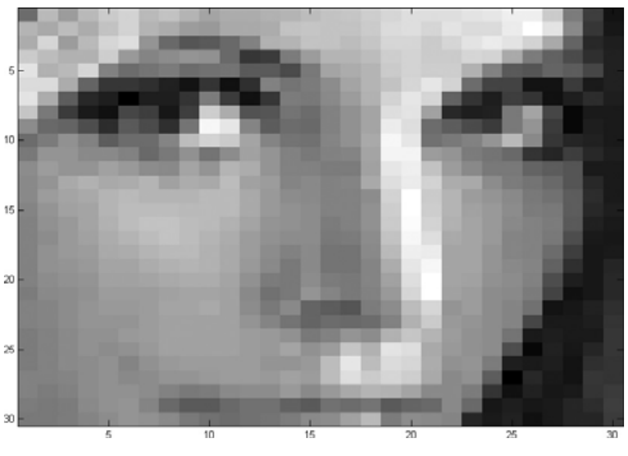

Fig. 18. Part of the Lena image (30 × 30 pixels).

The original image is shown in Fig. 18, and Figs. 19 and 20 show the image emerging from the chaos. Depending on the resolution and size of the image, there will come a point where further iterations will actually degrade the image as more and more of the unit square gets filled in.

An alternative to Bollt's affine function method, which rids the state-space structure of any self-similarity, is to map each rectangle $R_{\mathtt{ij}}$ onto the entire target partition element Q_j, and rotate the points in Q_j by $\pi/2$ radians.

$$\begin{aligned} \mathbf{f}_n^{\mathtt{ij}}(x,y) &= \begin{pmatrix} f_n^{\mathtt{ij}}(x) \\ g_n^{\mathtt{ij}}(y) \end{pmatrix} \\ &= \begin{pmatrix} 0 & \dfrac{\Delta y'_{\mathtt{ji}}}{\Delta y_{\mathtt{ji}}} \\ -1 & 0 \end{pmatrix} \cdot \begin{pmatrix} x - x_{\mathtt{ji}} \\ y - y_{\mathtt{ji}} \end{pmatrix} + \begin{pmatrix} x'_{\mathtt{ji}} \\ y'_{\mathtt{ji}} \end{pmatrix} \end{aligned} \tag{48}$$

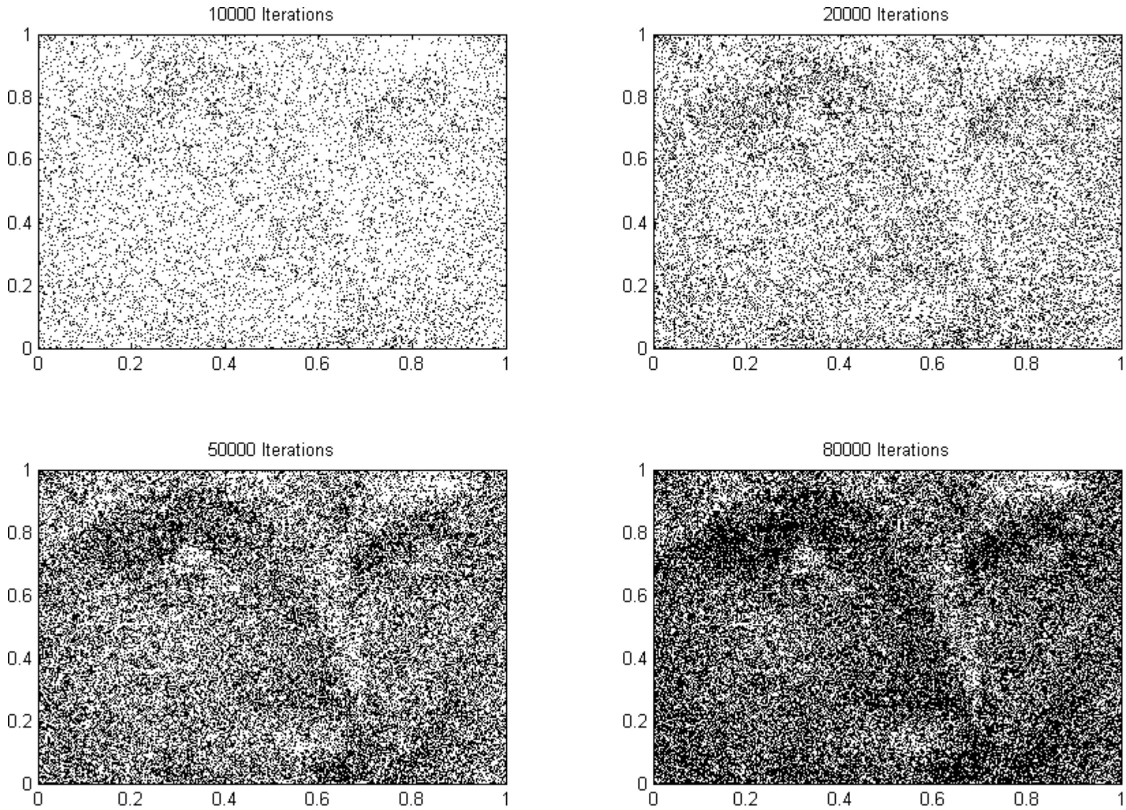

Fig. 19. Lena emerges as the map is iterated.

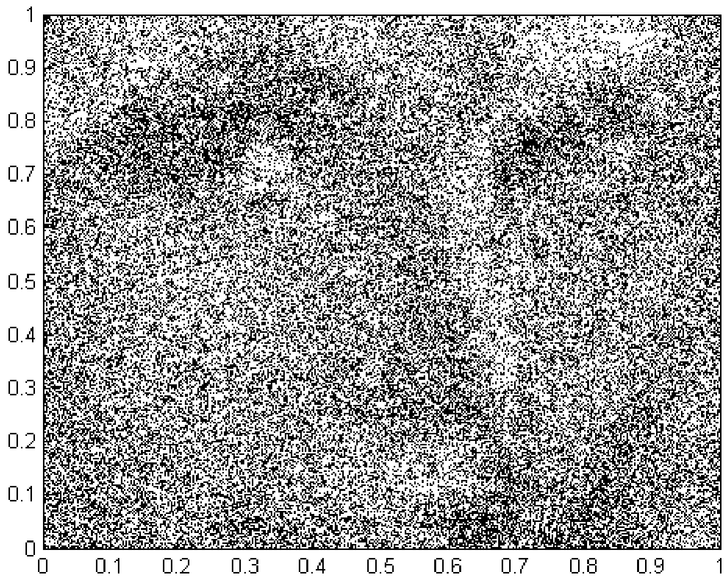

Fig. 20. 80000 iterations of the map.

Fig. 21. Noninvertible affine mapping with no self-similarity.

7. Conclusions

The Inverse Frobenius–Perron problem (IFPP) has achieved widespread attention in recent years as it offers a way of controlling the invariant density of chaotic maps, which in turn may lead to new ways to use chaos. In this paper, we described a matrix method which we have developed for solving the IFPP. In the method outlined, one has complete control over the map in terms of invariant density and autocorrelation function. The method described is straightforward and amenable to computer implementation. We also developed a closed form approximation for the autocorrelation and showed how it closely ties to expected values of autocorrelation. It was shown via simulation how the autocorrelation coefficients increase linearly with β. Modeling this variation will be a focus of our continuing work on these fascinating maps. The method described in the paper can be used to generate desired distributions of (quasi-) random numbers with desired decay of autocorrelation coefficients, or to model chaotic phenomena or time-series.

We also gave some fundamental results for a switched-chaotic map system, where one may obtain a desired invariant density by switching periodically or randomly among a set of piecewise linear maps. This class of positive matrices and associated chaotic maps possess many interesting properties, not least their parameterized solution to the inverse eigenvalue problem. Finally, we showed how the method could be extended to higher dimensions, and presented an interesting application of the IFPP by embedding an image into the invariant density of a chaotic map. We hope this paper will spur others into studying the theoretical and practical aspects of these systems.

Acknowledgments

This work was supported by the Irish Science and Technology Agency, Enterprise Ireland under research grant SC-00-86, and partially supported (R. Shorten) under grant SFI 04IN1I478.

References

Baranovsky, A. & Daems, D. [1995] "Design of one-dimensional chaotic maps with prescribed statistical properties," *Int. J. Bifurcation and Chaos* **5**, 1585–1598.

Berman, A., Shorten, R. & Leith, D. [2004] "Positive matrices associated with synchronised communication networks," *Lin. Algeb. Appl.* **393**, 47–54.

Bollt, E. M. [2000] "Controlling chaos and the inverse Frobenius–Perron problem: Global stabilization of arbitrary invariant measures," *Int. J. Bifurcation and Chaos* **10**, 1033–1050.

Box, G., Jenkins, G. & Reinsel, G. [1994] *Time Series Analysis*, 3rd edition (Prentice-Hall).

Boyarksy, A. & Góra, P. [1997] *Laws of Chaos* (Birkhäuser).

Boyarsky, A. & Góra, P. [2002] "Chaotic maps derived from trajectory data," *Chaos* **12**, 42–48.

Chen, G. & Dong, X. [1997] *From Chaos to Order* (World Scientific, Singapore).

Diakonos, F. *et al.* [1999] "A stochastic approach to the construction of one-dimensional chaotic maps with prescribed statistical properties," *Phys. Lett. A* **264**, 162–170.

Golub, G. & van Loan, C. [1996] *Matrix Computations* (Johns Hopkins University Press).

Gora, P. & Boyarsky, A. [1993] "A matrix solution to the inverse Frobenius–Perron problem," *Proc. Amer. Math. Soc.* **118**, 409–414.

Grossmann, S. & Thomae, S. [1977] "Invariant distributions and stationary correlation functions of one-dimensional discrete processes," *Zeitschrift für Naturforschung a* **32**, 1353–1363.

Horn, R. & Johnson, C. [1985] *Matrix Analysis* (Cambridge University Press).

Kocarev, L. [2001] "Chaos-based cryptography: A brief overview," *IEEE Circuits Syst. Mag.* **1**, 6–21.

Kohda, T. [2002] "Information sources using chaotic dynamics," *Proc. IEEE* **90**, 641–661.

Lasota, A. & Mackey, M. [1994] *Chaos, Fractals, and Noise*, Applied Mathematical Sciences, Vol. 97 (Springer-Verlag).

Li, T.-Y. [1976] "Finite approximation for the Frobenius–Perron operator: A solution to Ulam's conjecture," *J. Approx. Th.* **17**, 177–186.

Luenberger, D. G. [1979] *Introduction to Dynamic Systems* (Wiley).

Mondragon, R. J. [1999] "A model of packet traffic using a random wall model," *Int. J. Bifurcation and Chaos* **9**, 1381–1392.

Ott, E., Grebogi, C. & Yorke, J. [1990] "Controlling chaos," *Phys. Rev. Lett.* **64**, 1196–1199.

Ott, E. [2002] *Chaos in Dynamical Systems*, 2nd edition (Cambridge University Press).

Pareschi, F. *et al.* [2006] "A fast chaos-based true random number generator for cryptographic applications," *Proc. 32nd European Solid-State Circuits Conf.*, pp. 130–133.

Pingel, D. *et al.* [1999] "Theory and examples of the inverse-Frobenius–Perron problem for complete chaotic maps," *Chaos* **9**, 357–366.

Rogers, A., Shorten, R. & Heffernan, D. M. [2004] "Synthesizing chaotic maps with prescribed invariant densities," *Phys. Lett. A* **330**, 435–441.

Rogers, A., Shorten, R. & Heffernan, D. M. [2008] "A novel matrix approach for controlling the invariant densities of chaotic maps," *Chaos Solit. Fract.* **35**, 161–175.

Schuster, H. G. [1989] *Deterministic Chaos* (VCH).

Setti, G. *et al.* [2002] "Statistical modelling of discrete-time chaotic processes — basic finite-dimensional tools and applications," *Proc. IEEE* **90**, 662–690.

Shorten, R., Leith, D., Foy, J. & Kilduff, R. [2003] "Analysis and design of synchronised communication networks," *Proc. 12th Yale Workshop on Adaptive and Learning Systems*.

Strichartz, R. S. [2000] *The Way of Analysis* (Jones and Bartlett).

Tanenbaum, A. S. [2002] *Computer Networks*, 4th edition (Prentice-Hall).

Ulam, S. & von Neumann, J. [1947] "On combinations of stochastic and deterministic processes," *Bull. Amer. Math. Soc.* **53**, 1120.

Ulam, S. M. [1960] *A Collection of Mathematical Problems* (Interscience).

Wirth, F. *et al.* [2006] "Stochastic equilibria of AIMD communication networks," *SIAM J. Matrix Anal. Appl.* **28**, 703–723.